Hindawi
International Journal of Aerospace Engineering
Volume 2022, Article ID 6057998, 13 pages
https://doi.org/10.1155/2022/6057998

Research Article

Optimal Look-Angle Guidance with Field-of-View and Impact Angle Constraints for Strapdown Munition

Peng Wang,[1] **Jun-fang Fan**,[2] **Shi-wei Chen**,[1,2] **Hai-sen Wang**,[2] **and Wei Wang**[1]

[1]*School of Aerospace Engineering, Beijing Institute of Technology, Beijing 100081, China*
[2]*Beijing Key Laboratory of High Dynamic Navigation Technology, Beijing Information Science & Technology University, Beijing 100192, China*

Correspondence should be addressed to Jun-fang Fan; wyhffjf@bistu.edu.cn

Received 11 May 2022; Revised 14 July 2022; Accepted 5 August 2022; Published 29 August 2022

Academic Editor: Chen Pengyun

A strapdown seeker with limited field-of-view (FOV) can simplify and decrease cost of the guidance system for a munition. However, the inherent defect of the strapdown seeker is that it could not provide the necessary line-of-sight (LOS) angular information for typical guidance application. This paper proposed an optimal look-angle guidance law (OLAGL) which directly utilized seeker angle information and satisfies the constraints of FOV and terminal impact angle. The coefficient determination, effects of switching threshold, and gains for the guidance law are analyzed and detailed. The simulation results compared with typical trajectory shaping guidance for a ground target show that the presented guidance law can satisfy the impact angle constraint under the limitation of FOV and provide a well engineering reference.

1. Introduction

Compared with the gyro-stabilized seeker, a strapdown seeker is directly connected with the munition nose, which can omit the inertial platform and servo system and simplify the whole structure [1]. However, the strapdown seeker can only measure the angle between the munition axis and the line-of-sight (LOS), that is, the look-angle information, and fails measuring directly the LOS angular rate of the inertial coordinate. Meanwhile, the limited field-of-view (FOV) angle is also an obstacle. Therefore, the use of typical proportional navigation based guidance and advanced guidance laws are severely restricted for the strapdown seeker based munition and missile [2, 3]. Guidance, navigation, and control technology is widely used in spacecraft and munition control [4], and it is one of the key systems to perform various tasks [5].

For a missile against a nonmaneuvering target, a two-phased guidance problem with impact angle constraints and seeker's FOV limit was addressed in [6]. In [7], the relative motion relationship between munition and stationary target in pitch plane was established, and a suboptimal guidance law is deduced. Ref. [8] studied the guidance performance of the optimal guidance law for attacking low-velocity moving targets, introduced the time-to-go estimation method, and further designed the optimal guidance law that satisfies acceleration and impact angle. In [9], considering the dynamic lag effect and velocity change of munition, a generalized optimal guidance law with impact angle constraint was proposed. Ref. [10] deduced an optimal impact angle guidance law based on inscribed angle. Based on the sliding mode controller, ref. [11, 12] deduced the impact angle and time control guidance law, which made the actual look-angle can be stabilized at the expected look-angle. In [13], based on the estimation of minimum and maximum flight time and seeker limitation, a logical switching strategy of look-angle was proposed. Ref. [14] presented a compound guidance law combining sliding mode guidance with proportional guidance. In order to intercept a hypersonic target, in [15], a head-pursuit guidance law considering both the control system dynamics and the target maneuverability was presented via combining a fast power reaching law with backstepping sliding mode control.

Ref. [16] presented a shaping guidance law considering the impact angle of time-varying velocity and the FOV constraint, while the proposed guidance law was independent of constant velocity assumption and LOS rate information. In [17], a quadratic optimal function was constructed, and the look-angle guidance law was designed with small angle condition. In ref. [18], the optimal time and angle control guidance law were designed using the tracking error approach in finite time. For nonmaneuvering target, the closed-loop guidance law for controlling the relative look-angle on the virtual circle was derived in [19], which did not need the estimation of time-to-go. Ref. [20] proposed an optimal guidance law with terminal position and impact angle constraints and a new calculation method of time-to-go. In [21], the FOV angle change was regarded as inequality constraint, and the optimal impact angle guidance law was designed. [22] further introduced the range-to-go weighting function and analyzed the influence of different guidance weights on the guidance performance.

In this paper, considering the background of a shoulder strapdown guided munition with variable impact angle, the impact angle constraint problem is transformed into the normal velocity constraint by using the seeker angle information, which can save the steps of extracting the angular rate of the line of sight. The seeker's FOV is too narrow in the course of munition flight, and a generalized angle guidance law satisfying both the FOV angle and impact angle constraint is detailed, which is more practical and feasible in engineering.

The paper is organized as follows. Section 2 presents the munition-target dynamics model. Section 3 details the guidance law design. Section 4 analyzes the performance of guidance law on coefficient determination and comparative simulation. The conclusion is given in Section 5.

2. Munition-Target Dynamic Modelling

A theoretical model of shoulder strapdown guided munition vs. a moving target is shown in Figure 1.

Oxy represents inertial coordinate, M and T represent munition and target, respectively, FOV is the detecting range of the seeker, and r represents the LOS distance between munition M and target T. V and a_m are the velocity and acceleration of munition, α is the angle of attack, θ is the velocity inclination, ϑ is the pitch angle, σ is the look-angle, λ is the LOS angle, P is thrust, F is resistance, and is the gravity. The munition dynamics can be described as follows

$$m\frac{dV}{dt} = P - F - G\sin\theta, \tag{1}$$

$$\frac{dx}{dt} = V\cos\theta, \tag{2}$$

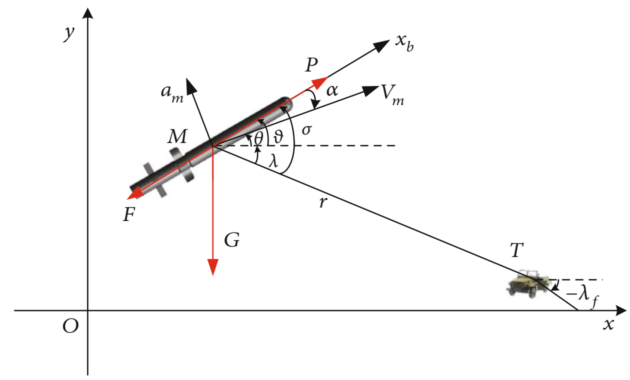

Figure 1: Geometric diagram of relative motion between munition-target.

$$\frac{dy}{dt} = V\sin\theta. \tag{3}$$

The relative motion between munition and target is

$$\dot{r} = -V\cos(\theta - \lambda), \tag{4}$$

$$r\dot{\lambda} = -V\sin(\theta - \lambda), \tag{5}$$

$$\dot{\theta} = \frac{a_m}{V}, \tag{6}$$

$$\vartheta = \alpha + \theta, \tag{7}$$

$$\sigma = \vartheta - \lambda. \tag{8}$$

3. Optimal Look-Angle Guidance Law Design

3.1. Basic Design without the FOV Angle Constraint. The following assumptions are made in this study:

(1) The munition velocity is constant

(2) The angle of attack is small and can be neglected

(3) The autopilot lag is ignored

Then, the munition motion can be represented as (which can be shown in Figure 2)

$$\begin{cases} \dot{y} = V\theta, \\ \ddot{y} = V\dot{\theta} = a_m, \end{cases} \tag{9}$$

where $\dot{y}$ and y represent the relative velocity and the normal displacement between the munition and the target, respectively. Equation (9) can be rewritten as state-space form

$$\dot{x} = Ax + Bu, \tag{10}$$

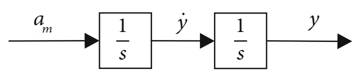

Figure 2: Dynamic model after linearization.

where $x = \begin{bmatrix} y \\ \dot{y} \end{bmatrix}$, $A = \begin{bmatrix} 0 & 1 \\ 0 & 0 \end{bmatrix}$, $B = \begin{bmatrix} 0 \\ 1 \end{bmatrix}$, $u = a_c$, and a_c are the acceleration command.

When the munition intercepts the target, the terminal relative velocity would be close to constant, and the distance between the impact point and the target is zero, then, the terminal constraint is satisfied

$$\begin{cases} y\left(t_f\right) = 0, \\ \dot{y}\left(t_f\right) = \dot{y}_f. \end{cases} \tag{11}$$

The power function of the time-to-go is introduced as the control function $S(t) = 1/(t_f - t)^n = 1/t_{\text{go}}^n$, $n \in \mathbb{R}^+$, n is the guidance order, t_{go} is the time-to-go, $t_{\text{go}} = t_f - t$, t_f is the terminal guidance time, and t is the current time. The objective function can be expressed as

$$\int_t^{t_f} S(t) a_c^2 dt = \int_t^{t_f} \frac{a_c^2}{t_{\text{go}}^n} dt, \tag{12}$$

where it is necessary to ensure $\lim_{t \longrightarrow t_f} a_c = 0$.

At the terminal time t_f, the general solution of the state space differential Eq. (10) can be expressed as

$$x\left(t_f\right) = W\left(t_f - t\right)x(t) + \int_t^{t_f} W\left(t_f - t\right)B(\eta)u(\eta)d\eta, \tag{13}$$

where W is the state transition matrix, i.e.,

$$\begin{aligned} x\left(t_f\right) &= L^{-1}\left[(sI - A)^{-1}\right]x(t) \\ &\quad + \int_t^{t_f} L^{-1}\left[(sI - A)^{-1}\right]\left(t_f - t\right)B(\eta)u(\eta)d\eta. \end{aligned} \tag{14}$$

Combining the coefficient matrices of the system, Eq. (14) can be expanded as follows

$$\begin{cases} y\left(t_f\right) = f_1 + \displaystyle\int_t^{t_f} e_1(\eta)a_c(\eta)d(\eta), \\ \dot{y}\left(t_f\right) = f_2^* + \displaystyle\int_t^{t_f} e_2(\eta)a_c(\eta)d(\eta), \end{cases} \tag{15}$$

where

$$\begin{cases} f_1 = y(t) + \left(t_f - t\right)\dot{y}(t), e_1(\eta) = \left(t_f - \eta\right)^{0.5n+1}, \\ f_2^* = \dot{y}(t), e_2(\eta) = \left(t_f - \eta\right)^{0.5n}. \end{cases} \tag{16}$$

Substituting the terminal constraint conditional Eq. (11) into Eq. (15), we can get

$$\begin{cases} f_1 = -\displaystyle\int_t^{t_f} e_1(\eta)a_c(\eta)d(\eta), \\ f_2^* - \dot{y}_f = -\displaystyle\int_t^{t_f} e_2(\eta)a_c(\eta)d(\eta) = -f_2. \end{cases} \tag{17}$$

Let the intermediate variable μ and combine the Eq. (17) to obtain

$$f_1 - \mu f_2 = -\int_t^{t_f} \left(e_1(\eta) + \mu e_2(\eta)\right)a_c(\eta)d\eta. \tag{18}$$

According to the objective function and Cauchy-Schwarz inequality

$$\int_t^{t_f} a_c^2(\eta)d\eta \geq \frac{\left(f_1 - \mu f_2\right)^2}{\int_t^{t_f}\left(e_1(\eta) - \mu e_2(\eta)\right)^2 d\eta}. \tag{19}$$

When the left side of Eq. (19) is equal to the right side, the objective function is minimal with value is Λ, i.e.,

$$\begin{aligned} \Lambda = \int_t^{t_f} a_c^2(\eta)d\eta &= \frac{\left(f_1 - \mu f_2\right)^2}{\int_t^{t_f}\left[e_1^2(\eta) - 2\mu e_1(\eta)e_2(\eta) + e_2^2(\eta)\right]d\eta} \\ &= \frac{\left(f_1 - \mu f_2\right)^2}{\left\|e_1^2\right\| - 2\mu\left\|e_1 e_2\right\| + \mu^2\left\|e_2^2\right\|}, \end{aligned} \tag{20}$$

where

$$\begin{cases} \left\|e_1^2\right\| = \displaystyle\int_t^{t_f} e_1^2(\eta)d\eta, \\ \left\|e_1 e_2\right\| = \displaystyle\int_t^{t_f} e_1(\eta)e_2(\eta)d\eta, \\ \left\|e_2^2\right\| = \displaystyle\int_t^{t_f} e_2^2(\eta)d\eta, \end{cases} \tag{21}$$

and we can get

$$a_c(\eta) = \zeta\left(e_1(\eta) - \mu e_2(\eta)\right), \tag{22}$$

where ζ is constant.

Considering Eqs. (20), (17), and (22), we can obtain

$$\zeta = \frac{f_1}{\left\|e_1^2\right\| - \mu\left\|e_1 e_2\right\|}. \tag{23}$$

When Λ is minimized, there is $d\Lambda/d\mu = 0$

$$\mu = \frac{f_1\left\|e_1 e_2\right\| - f_2\left\|e_1^2\right\|}{f_1\left\|e_2^2\right\| - f_2\left\|e_1 e_2\right\|}. \tag{24}$$

Table 1: Initial condition.

Initial munition position	Munition flight velocity	Initial trajectory inclination	Initial target position	Target velocity
(0, 0.7) m	(240, 0) m/s	3°	(3, 500, 0) m	(10, 0) m/s

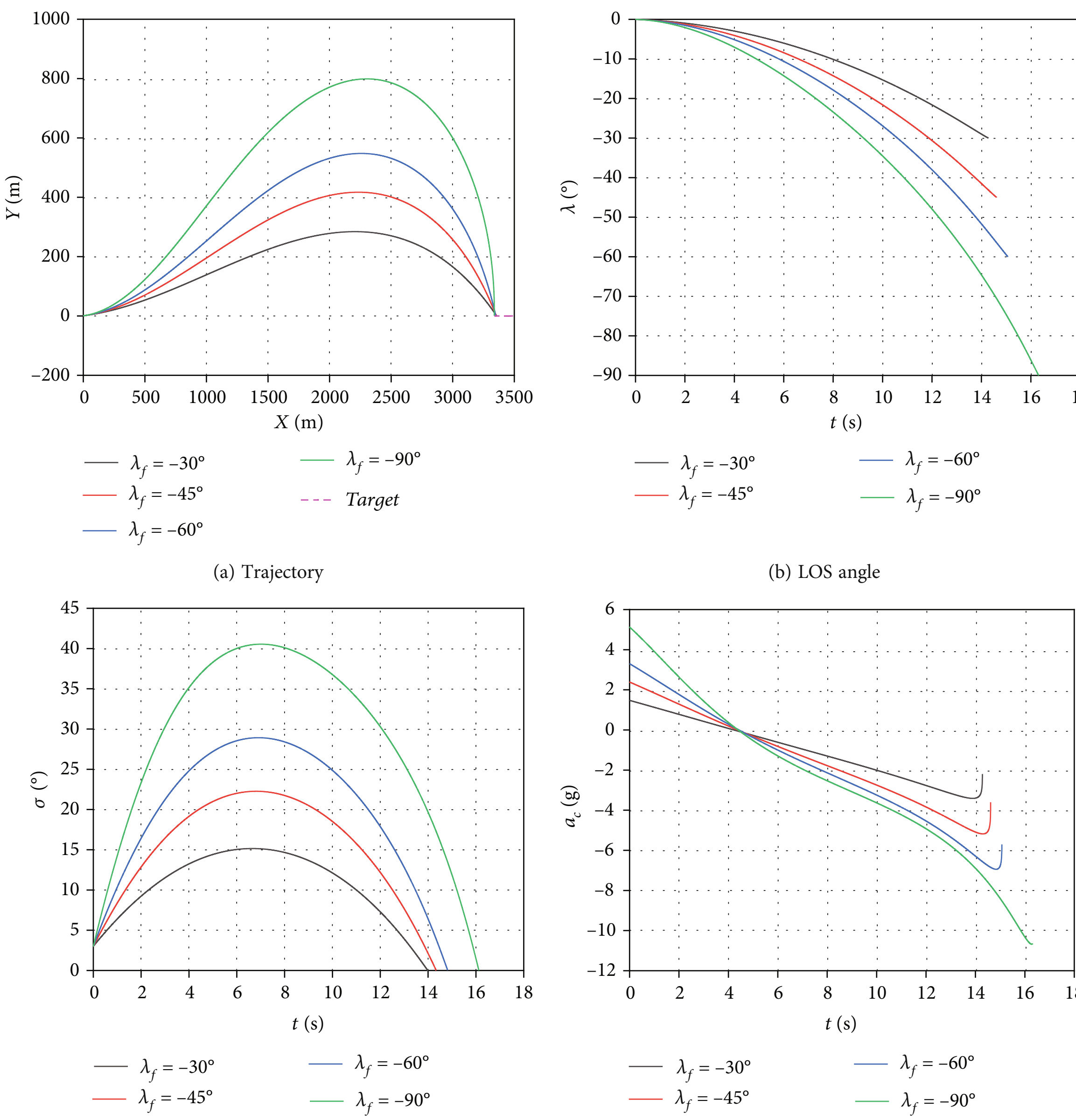

(a) Trajectory (b) LOS angle (c) Look-angle (d) Acceleration

Figure 3: The results of different impact angles without FOV constraints.

Table 2: Guidance laws with different guidance coefficients.

N_σ	N_λ	Guidance law
4	2	$a_c(t) = -\left(V/t_{go}\right)\left[4\sigma + 2\left(\lambda_f - \lambda\right)\right]$
6	6	$a_c(t) = -\left(V/t_{go}\right)\left[6\sigma + 6\left(\lambda_f - \lambda\right)\right]$
8	12	$a_c(t) = -\left(V/t_{go}\right)\left[8\sigma + 12\left(\lambda_f - \lambda\right)\right]$

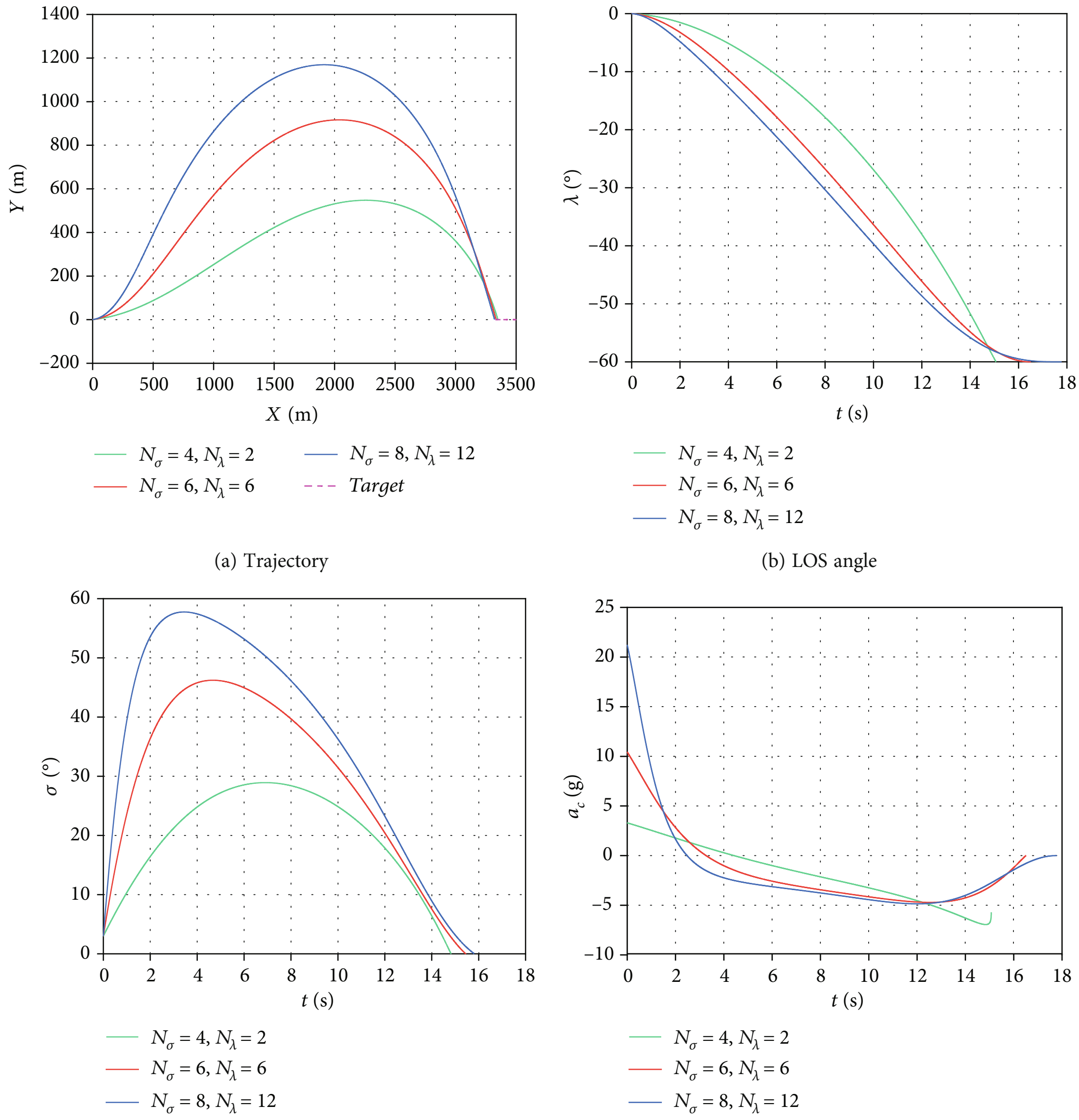

Figure 4: The results of different guidance coefficients without FOV constraints.

Table 3: Guidance coefficients.

N_σ	N_λ	σ_{max}	σ_s	k	k_2
4	2	15°	10°	0.05	1.5

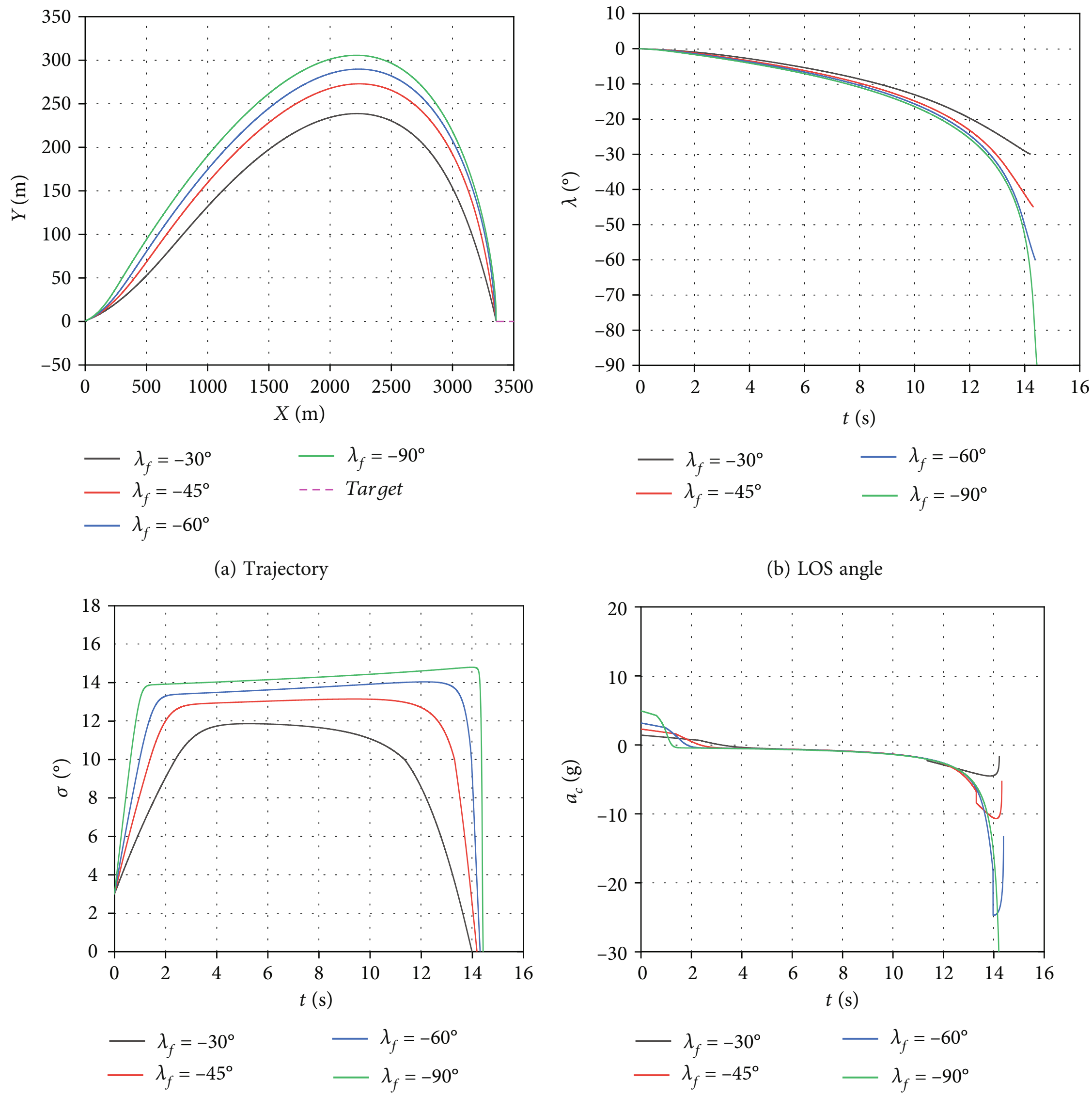

(a) Trajectory

(b) LOS angle

(c) Look-angle

(d) Acceleration

Figure 5: The results of different impact angles considering FOV constraints.

Then, at any time t, there is

$$a_c(t) = \frac{f_1 e_1(t)\left\|e_2^2\right\| - \left(f_1 e_2(t) + f_2 e_1(t)\right)\left\|e_1 e_2\right\| + f_2 e_2(t)\left\|e_1^2\right\|}{\left\|e_1^2\right\|\left\|e_2^2\right\| - \left\|e_1 e_2\right\|^2}. \tag{25}$$

where

$$\begin{cases} f_1 = y + (t_f - t)\dot{y} = y + t_{go}\dot{y}, & \left\|e_1^2\right\| = \int_t^{t_f} e_1^2(t)d\eta = \int_t^{t_f} t_{go}^{2(0.5n+1)}d\eta = \dfrac{t_{go}^{n+3}}{n+3}, \\ f_2 = \dot{y} - \dot{y}(t_f), & \\ e_1(t) = (t_f - t)^{0.5n+1} = t_{go}^{0.5n+1}, & \left\|e_1 e_2\right\| = \int_t^{t_f} e_1(t)e_2(t)d\eta = \int_t^{t_f} t_{go}^{n+1}d\eta = \dfrac{t_{go}^{n+2}}{n+2}, \\ e_2(t) = (t_f - t)^{0.5n} = t_{go}^{0.5n}, & \left\|e_2^2\right\| = \int_t^{t_f} e_2^2(t)d\eta = \int_t^{t_f} t_{go}^{n}d\eta = \dfrac{t_{go}^{n+1}}{n+1}. \end{cases} \tag{26}$$

Let

$$\begin{cases} N_{12} = (n+1)(n+2), \\ N_{22} = 2(n+2), \\ N_{32} = (n+2)(n+3). \end{cases} \tag{27}$$

The acceleration command can be further obtained as follows

$$a_c(t) = -\frac{1}{t_{go}^2}\left(N_{32}y + N_{22}t_{go}\dot{y} + N_{12}t_{go}\dot{y}_f\right). \tag{28}$$

The strapdown seeker can only measure the angle information during flight, so it is necessary to give the command containing only the direct measurement information for (28).

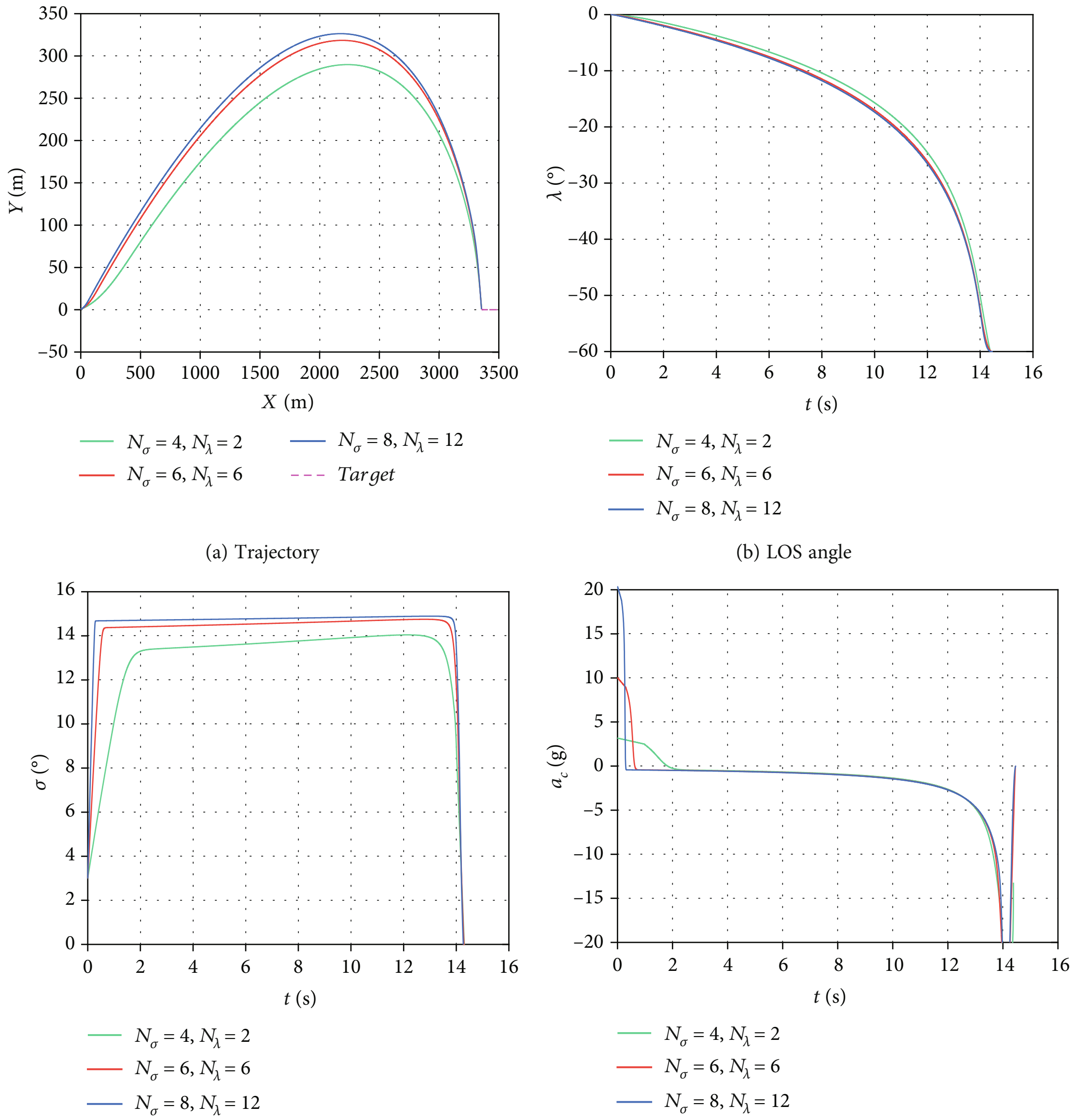

(a) Trajectory

(b) LOS angle

(c) Look-angle

(d) Acceleration

Figure 6: The results of different guidance coefficients considering FOV constraints.

Under the small-angle linearization model, the LOS angle can be expressed as

$$\lambda = -\frac{y}{r} = -\frac{y}{V_r t_{go}}. \tag{29}$$

According to Eqs. (7)–(9) and $r = V_r t_{go}$, we can get

$$\dot{y} = V_r \theta = V_r \sigma + V_r \lambda. \tag{30}$$

It satisfies at the terminal

$$\dot{y}_f = V_r \lambda_f, \tag{31}$$

where V_r is the relative velocity between the munition and the target and equal to the flight velocity of the munition for a stationary target or a moving target with a low velocity. By substituting Eqs. (29)–(31) into Eq. (28), the guidance command only containing the measurement angle information and the terminal angle constraint can be obtained as follows

$$a_c(t) = -\frac{V}{t_{go}} \left[N_\sigma \sigma + N_\lambda \left(\lambda_f - \lambda \right) \right], \tag{32}$$

where N_λ and N_σ are guidance coefficients and equal to N_{12} and N_{22} in Eq. (27). This is the formula of the proposed optimal look-angle guidance law (OLAGL).

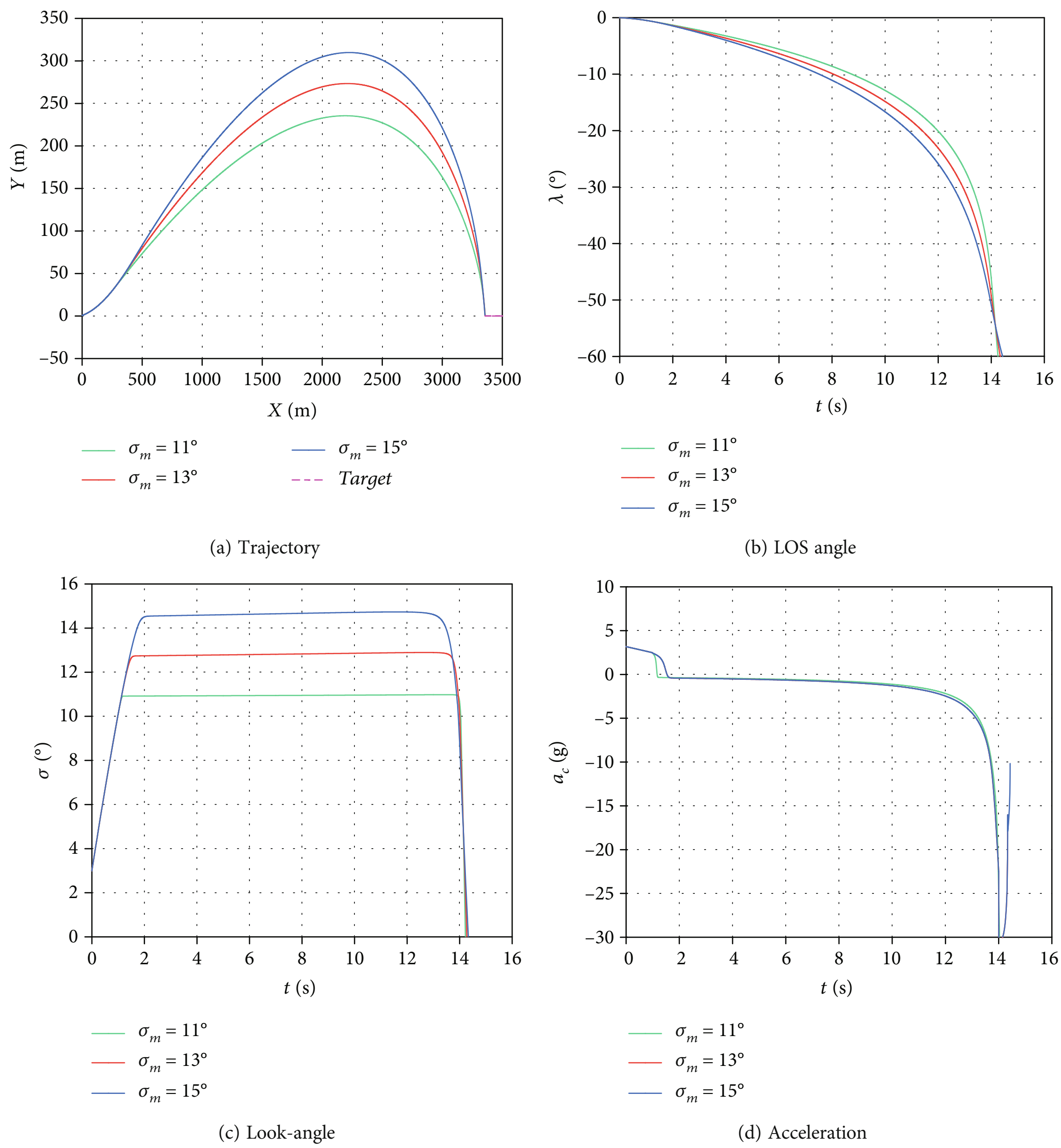

(a) Trajectory

(b) LOS angle

(c) Look-angle

(d) Acceleration

FIGURE 7: The results considering different FOV constraints.

3.2. Advanced Design considering the FOV Constraint. The terminal impact angle requirement for efficient strike and the limited FOV of strapdown seeker propose a great challenge for look-angle guidance. Therefore, it is necessary to take into consideration the FOV constraint on the aforementioned designed OLAGL.

It can be seen from Figure 1, ignoring the small angle of attack, the seeker look-angle σ can be obtained as follows

$$\sigma = \theta - \lambda. \tag{33}$$

The design philosophy with FOV constraint is make seeker's look-angle within its maximal σ_m. During the flight, the look-angle range of a strapdown seeker varies along the attitude and distance between munition and target. Given an additional correction term that is opposite to the varied direction of the look-angle, the look-angle will converge. Therefore, the guidance command with correction term can be designed as follows

$$\Delta a_c = k \operatorname{sgn}(\sigma) \frac{|\sigma| - \sigma_s}{|\sigma| - \sigma_m}. \tag{34}$$

Thus, the OLAGL with FOV and impact angle constraint is obtained as follows

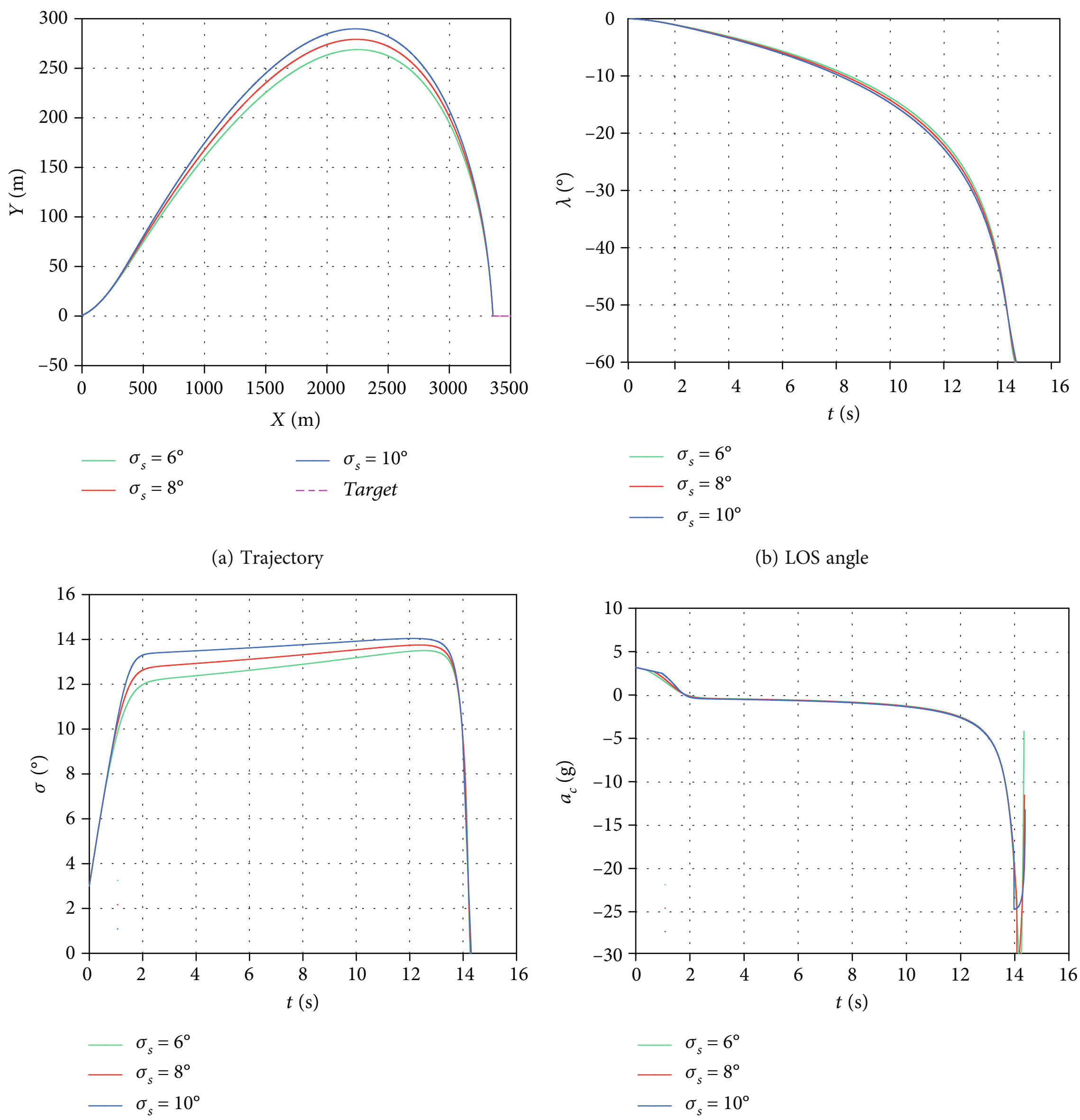

(a) Trajectory
(b) LOS angle
(c) Look-angle
(d) Acceleration

FIGURE 8: The results considering different switching thresholds.

where σ_s is the switching threshold, k is the switching gain coefficient, and k_2 is the gravity compensation coefficient. When the look-angle is larger than the switching threshold, a correction term is acted, and the FOV constraint guidance law is adopted to pull the look-angle backward within the limited range. Otherwise, the basic OLAGL is performed. The addition term of $|\sigma| - \sigma_m$ is benefit to decrease the acceleration requirement, so as to prevent drastic jump when the

$$a_c(t) = \begin{cases} -\dfrac{V}{t_{\text{go}}}\left[N_\sigma \sigma + N_\lambda\left(\lambda_f - \lambda\right)\right] + k_2 g \cos(\theta), & |\sigma| < \sigma_s, \\ -\dfrac{V}{t_{\text{go}}}\left[N_\sigma \sigma + N_\lambda\left(\lambda_f - \lambda\right)\right] + k \operatorname{sgn}(\sigma)\dfrac{|\sigma| - \sigma_s}{|\sigma| - \sigma_m} + k_2 g \cos(\theta), & \sigma_s \le |\sigma| < \sigma_m. \end{cases} \tag{35}$$

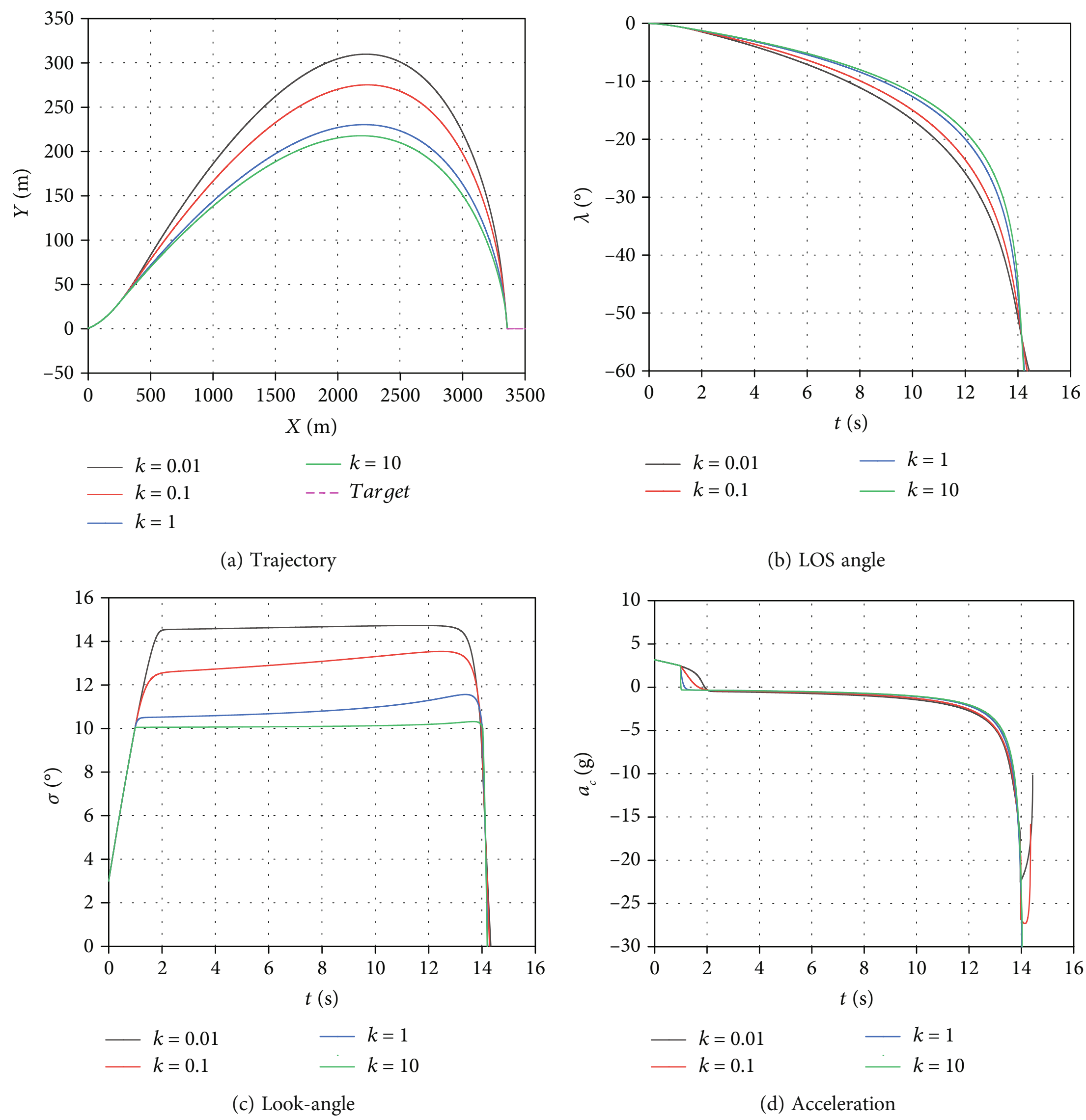

FIGURE 9: The results considering different switching gains.

correction term is introduced and improve the tracking stability of the seeker.

4. Simulation and Analysis

4.1. The OLAGL without FOV Constraints

4.1.1. Considering Impact Angle Constraint. The simulation conditions are shown in Table 1.

The guidance coefficient is $N_\sigma = 4$ and $N_\lambda = 2$. The simulation results are shown in Figure 3.

When the expected impact angle is larger, the trajectory will climb to a higher position to meet the impact angle, and the flight time will be longer, resulting in a large terminal acceleration. Without considering the FOV constraint, the seeker's look-angle gradually increases at the initial stage, but the range of look-angle remains within 40°. Therefore, the constraint of impact angle should be analyzed for the engineering application.

4.1.2. Considering Different Guidance Coefficients. Given $\lambda_f = -60^\circ$ as the case, the effect of guidance coefficients is analyzed as Table 2. The simulation results are shown in Figure 4.

The results show that for a given impact angle, the munition can intercept the target with different guidance coefficients. The larger the guidance coefficient, the more steeper the flight trajectory, the larger the seeker's look-angle and the miss distance, the longer it takes to intercept the target. If the munition acceleration is limited, the acceleration saturation will occur at the end, which will result in obvious miss distance. If the coefficient meets $N_\sigma > 4$ and $N_\lambda > 2$, a larger acceleration command is required at the initial stage.

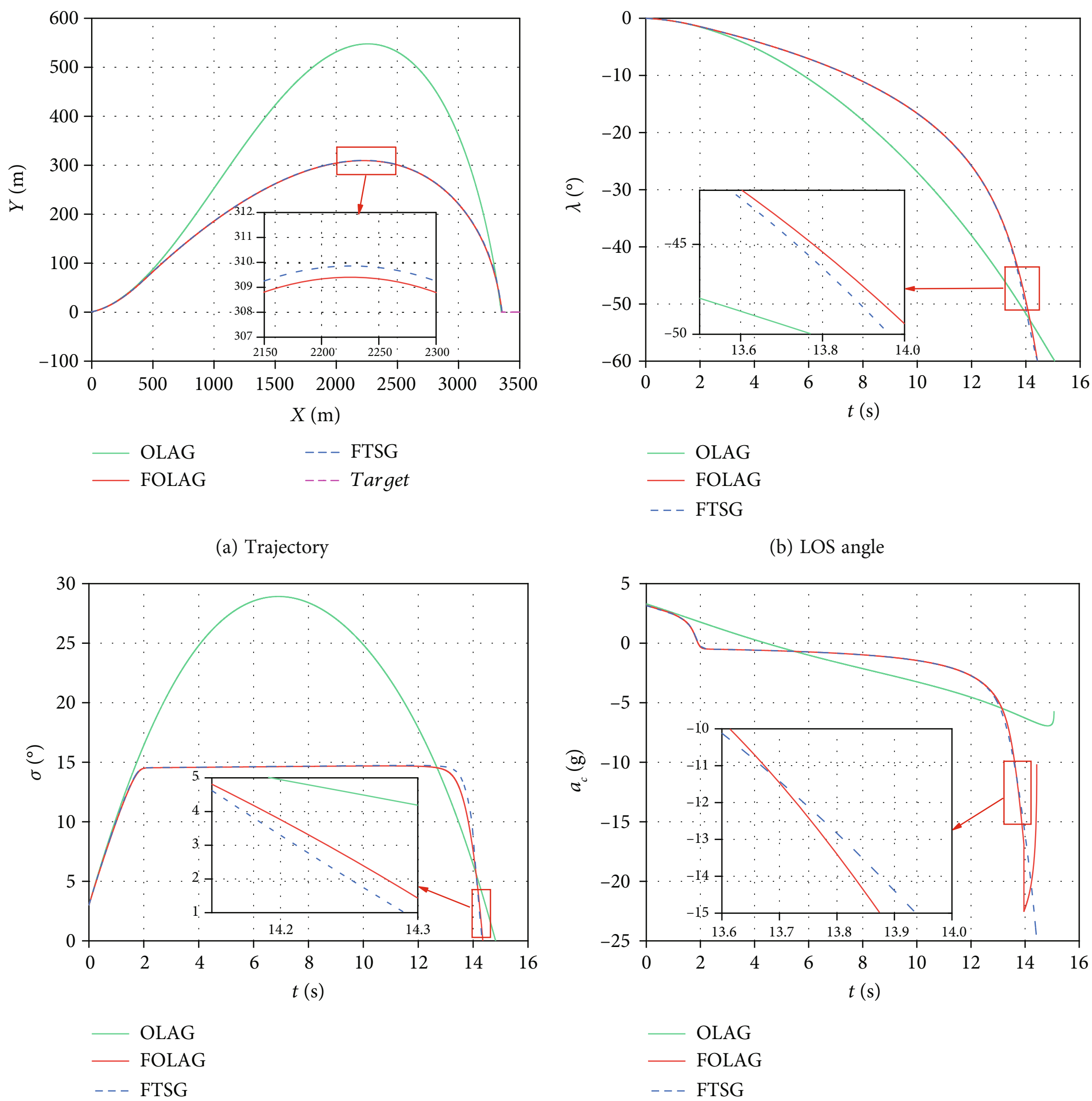

(a) Trajectory (b) LOS angle (c) Look-angle (d) Acceleration

Figure 10: The comparison results of different guidance law.

4.2. The OLAGL considering FOV Constraint

4.2.1. Considering FOV Constraint under Different Impact Angles. The initial information of munition and moving target is as mentioned in Part 4.1, and other coefficients are selected as in Table 3.

Considering different impact angles, the results are shown in Figure 5. It can be seen the designed OLAGL considering the FOV constraint can make the munition intercept the target precisely, while the LOS angle is constrained to the desired impact angle. With the increase of the impact angle, the trajectory keeps smooth, and the look-angle always remains within the limited range until intercepting the target.

4.2.2. Considering FOV Constraint with Different Guidance Coefficients. Given $\lambda_f = -60^\circ$ and the maximum FOV is 15° as the case, the guidance coefficients are analyzed. The simulation results are shown in Figure 6.

It can be seen that the guidance laws formed by different guidance coefficients can meet the impact angle under the constraint of FOV. The smaller the guidance coefficient, the shorter the interception time and the smaller the acceleration command. Besides, when the FOV constraint is added, the trajectory height varies a little compared with the guidance coefficient.

4.2.3. Considering Different FOV Constraints. Let coefficients $N_\sigma = 4$, $N_\lambda = 2$, and $\lambda_f = -60^\circ$ as the case. For different maximal value of FOV angle, the simulation results are shown in Figure 7.

When the look-angle constraint is smaller, the trajectory is smoother, while the required terminal acceleration is greater. A wide FOV range is benefit for application.

4.2.4. Considering Different Switching Thresholds. Given the coefficients $N_\sigma = 4$ and $N_\lambda = 2$, $\lambda_f = -60^\circ$, and the maximum FOV is 15° as the case. For different look-angle switching threshold, the simulation results are shown in Figure 8.

4.2.5. Considering Different Switching Gains. Let the switching threshold of the look-angle is 10°. For different switching gain coefficient, the simulation results are shown in Figure 9.

The simulation results show that the switching gain of the correction term has great effect on the flight performance. A large switching gain results in strong correction effect and more smooth trajectory.

4.2.6. Comparative Analysis. Considering the typical trajectory shaping guidance law with FOV constraints as the reference, a comparison analysis of the guidance performance is detailed in this part. For convenience, the proposed OLAGL without and with FOV constraint is abbreviated as OLAG and FOLAG, and the trajectory shaping guidance law with FOV constraint in the literature is FTSG, respectively. The simulation results are shown in Figure 10.

It can be seen that all three guidance laws can meet the requirements of interception and impact angle constraint, and the FOLAG has the best effect on impact angle and trajectory control. Besides, the trajectory from the FOLAG and the FTSG is more smoothly than that of the OLAG, which shows the importance of adding a look-angle constraint. Besides, compared with the FSTG, the FOLAG changes more smoothly, and the terminal guidance command is smaller.

5. Conclusion

This paper detailed an optimal look-angle guidance law (OLAGL) with look-angle and impact angle constraints which directly utilized the angle information of the strapdown seeker. The coefficient determination and effect on guidance performance were analyzed. The feasibility of the proposed guidance law was verified by numerical simulation and comparative analyse. The results showed that the proposed OLAGL omitted the extraction of LOS angle rate and could satisfy the guidance precision requirement under constraints. Therefore, the proposed guidance law was practicable in engineering.

Data Availability

No data is provided in this article.

Conflicts of Interest

The authors declare that they have no conflicts of interest.

Acknowledgments

This work is supported in part by the National Key Research & Development Program under Grant no. 2020YFC1511705 and the National Natural Science Foundation of China under Grant no. 61801032.

References

[1] H. K. Woo, "Stability analysis of strapdown seeker scale-factor error and LOS rate," *In Proceeding of the AIAA Guidance, Navigation and Control Conference*, vol. 6788, pp. 115–122, 2007.

[2] S. A. Jang, C. K. Ryoo, K. Choi, and M. J. Tahk, "Guidance algorithms for tactical missiles with strapdown seeker," in *2008 SICE Annual Conference*, pp. 2616–2619, Chofu, Japan, 2008.

[3] D. Kim, C. K. Ryoo, Y. Kim, and J. Kim, "Guidance and control for missiles with a strapdown seeker," in *2011 11th International Conference on Control, Automation and Systems*, pp. 960–972, Gyeonggi-do, Korea (South), 2011.

[4] X. Y. Huang, M. D. Li, X. L. Wang et al., "The tianwen-1 guidance, navigation, and control for mars entry, descent, and landing," *Space: Science & Technology*, vol. 2021, article 9846185, 13 pages, 2021.

[5] H. H. Zhang, J. Li, Z. G. Wang, and Y. Guan, "Guidance navigation and control for chang'E-5 powered descent," *Space: Science & Technology*, vol. 2021, Article ID 9823609, 15 pages, 2021.

[6] H. Q. Zhang, S. J. Tang, J. Guo, and W. Zhang, "A two-phased guidance law for impact angle control with seeker's field-of-view limit," *International Journal of Aerospace Engineering*, vol. 2018, Article ID 7403639, 13 pages, 2018.

[7] M. K. Kim and V. Grider, "Terminal guidance for impact attitude angle constrained flight trajectories," *IEEE Transactions on Aerospace and Electronic Systems*, vol. 6, pp. 852–859, 1973.

[8] C. K. Ryoo, H. Cho, and M. J. Tahk, "Optimal guidance laws with terminal impact angle constraint," *Journal of Guidance, Control & Dynamics*, vol. 28, no. 4, pp. 724–732, 2005.

[9] C. H. Lee and M. Y. Ryu, "Practical generalized optimal guidance law with impact angle constraint," *Proceedings of the Institution of Mechanical Engineering*, vol. 233, no. 10, pp. 3790–3809, 2019.

[10] R. Tsalik and T. Shima, "Optimal guidance around circular trajectories for impact-angle interception," *Journal of Guidance Control & Dynamics*, vol. 39, no. 6, pp. 1278–1291, 2016.

[11] H.-G. Kim and H. J. Kim, "Impact time control guidance considering seeker's field-of-view limits," in *2016 IEEE 55th Conference on Decision and Control (CDC)*, Las Vegas, NV, USA, 2016.

[12] H. G. Kim, J. Y. Lee, H. J. Kim, H. H. Kwon, and J. S. Park, "Look-angle-shaping guidance law for impact angle and time control with field-of-view constraint," *IEEE Transactions on Aerospace and Electronic Systems*, vol. 56, no. 2, pp. 1602–1612, 2020.

[13] D. K. Sang and M. J. Tahk, "Guidance law switching logic considering the seeker's field-of-view limits," *Proceedings of the Institution of Mechanical Engineers Part G-Journal of Aerospace Engineering*, vol. 223, no. 8, pp. 1049–1058, 2009.

[14] C. H. Lee, C. Hyun, J. G. Lee, J. Y. Choi, and S. Sung, "A hybrid guidance law for a strapdown seeker to maintain lock-on conditions against high speed targets," *Journal of Electrical Engineering and Technology*, vol. 8, no. 1, pp. 190–196, 2013.

[15] C. Q. Zhu and Z. Y. Guo, "Design of head-pursuit guidance law based on backstepping sliding mode control," *International Journal of Aerospace Engineering*, vol. 2019, Article ID 8214042, 18 pages, 2019.

[16] Q. Hu, R. Cao, T. Han, and M. Xin, "Field-of-view limited guidance with impact angle constraint and feasibility analysis," *Aerospace Science and Technology*, vol. 114, no. 1, article 106753, 2021.

[17] J. F. Fan, W. Gang, C. Ying, and D. Si-yu, "Impact-angle-constraint look angle guidance for miniature missile," in *2016 16th*

International Conference on Control, Automation and Systems (ICCAS), Gyeongju, Korea (South), 2016.

[18] B. Li, D. F. Lin, S. M. He, and B. Bai, "Time and angle control guidance law based on optimal error dynamics," *Acta Aeronautica et Astronautica Sinica*, vol. 39, no. 11, pp. 157–167, 2018.

[19] I. S. Jeon and M. Karpenko, "Off-target look angle control guidance law for moving targets," *Journal of Guidance Control & Dynamics*, vol. 42, no. 11, pp. 2432–2442, 2019.

[20] C. K. Ryoo, H. Cho, and M. J. Tahk, "Time-to-go weighted optimal guidance with impact angle constraints," *IEEE Transactions on Control Systems Technology*, vol. 14, no. 3, pp. 483–492, 2006.

[21] B. G. Park, T. H. Kim, and M. J. Tahk, "Optimal impact angle control guidance law considering the seeker's field-of-view limits," *Proceedings of Institution of Mechanical Engineers Part G Journal of Aerospace Engineering*, vol. 227, no. 8, pp. 1347–1364, 2013.

[22] B. G. Park, T. H. Kim, and M. J. Tahk, "Range-to-go weighted optimal guidance with impact angle constraint and seeker's look angle limits," *IEEE Transactions on Aerospace and Electronic Systems*, vol. 52, no. 3, pp. 1241–1256, 2016.